Journal of Colloid and Interface Science 488 (2017) 225–233

Contents lists available at ScienceDirect

Journal of Colloid and Interface Science

journal homepage: www.elsevier.com/locate/jcis

Lubrication synergy: Mixture of hyaluronan and dipalmitoylphosphatidylcholine (DPPC) vesicles

Akanksha Raj [a], Min Wang [a], Thomas Zander [b], D.C. Florian Wieland [b], Xiaoyan Liu [a,1], Junxue An [a], Vasil M. Garamus [b], Regine Willumeit-Römer [b], Matthew Fielden [c], Per M. Claesson [a,d], Andra Dėdinaitė [a,d,*]

[a] KTH Royal Institute of Technology, School of Chemical Sciences and Engineering, Department of Chemistry, Surface and Corrosion Science, Drottning Kristinas Väg 51, SE-10044 Stockholm, Sweden
[b] Helmholtz Zentrum Geesthacht, Institute for Materials Research, Max-Planck Straße 1, 21502 Geesthacht, Germany
[c] KTH Royal Institute of Technology, Albanova Campus, Department of Applied Physics, Roslagstullsbacken 21, SE-10044 Stockholm, Sweden
[d] SP Technical Research Institute of Sweden, SP Chemistry, Materials and Surfaces, Box 5607, SE-114 86 Stockholm, Sweden

GRAPHICAL ABSTRACT

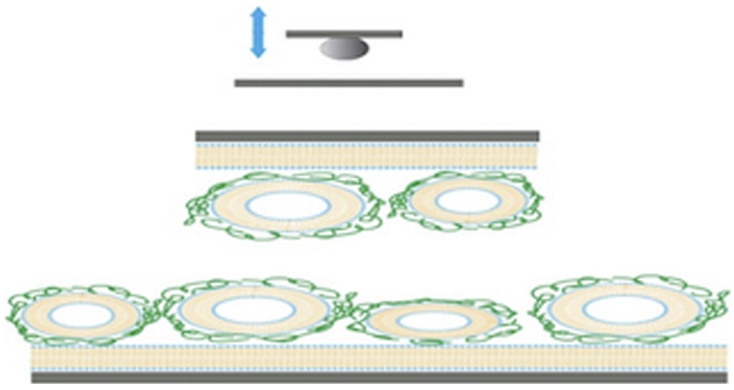

ARTICLE INFO

Article history:
Received 1 September 2016
Revised 28 October 2016
Accepted 31 October 2016
Available online 1 November 2016

Keywords:
Dipalmitoylphosphatidylcholine (DPPC)
Hyaluronan
Adsorption
Self-assembly
QCM-D

ABSTRACT

Phospholipids and hyaluronan have been implied to fulfil important roles in synovial joint lubrication. Since both components are present in synovial fluid, self-assembly structures formed by them should also be present. We demonstrate by small angle X-ray scattering that hyaluronan associates with the outer shell of dipalmitoylphophatidylcholine (DPPC) vesicles in bulk solution. Further, we follow adsorption to silica from mixed hyaluronan/DPPC vesicle solution by Quartz Crystal Microbalance with Dissipation measurements. Atomic Force Microscope imaging visualises the adsorbed layer structure consisting of non-homogeneous phospholipid bilayer with hyaluronan/DPPC aggregates on top. The presence of these aggregates generates a long-range repulsive surface force as two such surfaces are brought together. However, the aggregates are easily deformed, partly rearranged into multilayer structures and partly removed from between the surfaces under high loads. These layers offer very low friction coefficient (<0.01), high load bearing capacity (≈23 MPa), and self-healing ability. Surface bound DPPC/

* Corresponding author at: Department of Chemistry, Surface and Corrosion Science, Drottning Kristinas Väg 51, SE-10044 Stockholm, Sweden.
E-mail addresses: rajaka@kth.se (A. Raj), mwang@kth.se (M. Wang), thomas.zander@hzg.de (T. Zander), florian.wieland@hzg.de (D.C.F. Wieland), liuxia@kemi.dtu.dk (X. Liu), junxue@kth.se (J. An), vasyl.haramus@hzg.de (V.M. Garamus), regine.willumeit@hzg.de (R. Willumeit-Römer), fielden@kth.se (M. Fielden), percl@kth.se (P.M. Claesson), andra@kth.se (A. Dėdinaitė).
[1] Present address: Technical University of Denmark, Department of Chemistry, Kemitorvet 207, DK-2800 KGs. Lyngby, Denmark.

http://dx.doi.org/10.1016/j.jcis.2016.10.091
0021-9797/

AFM imaging
Surface forces
Friction
Lubrication
Small-angle X-ray scattering

hyaluronan aggregates provide a means for accumulation of lubricating DPPC molecules on sliding surfaces.

1. Introduction

The smooth motion of synovial joints has intrigued scientists for years. This has inspired work to understand the nanomechanical properties of the hierarchical and nanostructured cartilage surface [1], identify the important biolubricants [2], and develop biomimetic lubricants that can provide low friction and high load bearing capacity between sliding surfaces in aqueous solutions [3,4]. It is now well understood that key biolubricants include phospholipids, hyaluronan [5,6], and glycoproteins (like lubricin) with an overall bottle-brush structure [7]. We suggest that the outstanding performance of the synovial joint is not due to the properties of any single biolubricant, but the key is to understand synergism in mixtures containing the different components [2,8,9]. In this report we focus on two components, hyaluronan and dipalmitoylphosphatidylcholine, but emphasize the natural biolubrication system is significantly more complex and utilizes also other biolubricants.

Hyaluronan is a linear anionic polysaccharide present in the synovial fluid at a concentration of 1.4–3.1 g/L [10]. It consists of repeating D-glucuronic acid and *N*-acetyl-glucosamine units connected via alternating $\beta_{1,3}$ and $\beta_{1,4}$ glycosidic bonds. The pK_a of D-glucuronic acid is about 3.3 [11]. Hyaluronan alone does not provide any exceptionally low friction force between model surfaces [12]. However, in association with phospholipids, hyaluronan is a potent lubricant [13]. Dipalmitoylphosphatidylcholine, DPPC, is an abundant saturated phospholipid found in the synovial fluid [14,15]. The phase transition temperature for DPPC in contact with bulk water is 41 °C. Above this temperature DPPC is in the liquid crystalline phase and thus the acyl chains are fluid-like, whereas below this temperature they are solid-like in the gel phase. A ripple phase has also been reported to exist between the gel and liquid crystalline phases [16]. Recently, the structure of DPPC bilayers deposited at the silica-aqueous interface was characterised both in the fluid and gel state using X-ray reflectivity measurements [17]. We have previously shown that sequential adsorption of DPPC and hyaluronan can build a composite layer that allows a large amount of phospholipid to be present on the surface, and this layer provides low friction and high load bearing capacity on silica surfaces [6].

It is, however, difficult to see how sequential adsorption would occur in a biological environment. It is more likely that the components forming the adsorbed layer will be present in the solution and may form self-assembly aggregates that attach to the surface. In this work we explore the adsorption and lubrication performance of self-assembled aggregates, by studying adsorption from a 155 mM NaCl solution containing equal mass concentrations of hyaluronan and DPPC onto silica surfaces. The self-assembly structure formed in mixed hyaluronan and DPPC vesicle solutions was investigated by small angle X-ray scattering. The adsorption process was monitored by QCM-D, and the morphology of the layer was probed by AFM imaging. Surface and friction forces were determined with the AFM colloidal probe technique. We found that the layers formed by adsorption from mixed DPPC/hyaluronan solutions were less well ordered than the DPPC bilayers formed in absence of hyaluronan. However, the mixed layers were able to sustain high loads and sliding was characterized by a very low friction coefficient. It was also noted that low friction was recovered after structural rearrangements induced by the combined action of load and shear, suggesting a self-healing ability.

2. Materials and methods

2.1. Materials

1,2-Dipalmitoyl-*sn*-glycero-3-phosphocholine (DPPC) was purchased from Avanti Polar Lipids (catalogue No. 850355P, Avanti, USA) in powder form and used as received. Hyaluronan with an average molecular weight M_w of 6.2×10^5 g/mol was a kind gift from Novozymes (Denmark), and the molecular weight distribution, $M_w/M_n = 1.9$, was characterized by means of asymmetric flow flow-field fractionation, AFFFF by Postnova analytics GmbH. Sodium chloride (ACS reagent, assay ⩾ 99.0%) and chloroform (ACS assay ⩾ 99.5%, catalogue No.C2432) were purchased from Sigma-Aldrich (USA). The water used in all experiments was purified by a Millipore system consisting of a Milli-Q Integral 15 unit, including a final 0.22 μm Millipak filter. The purified water had a resistivity of 18.2 MΩ cm at 25 °C, and the total organic carbon content was less than 3 ppb. Silicon wafers with a 100 nm thick SiO_2 layer (Wafernet, Germany) were used as flat substrates in AFM studies. They were, prior to experiment, cut into size of 13×13 mm^2, and then cleaned by immersion into 2% Hellmanex solution (Hellma, USA) for 30 min. Next, they were rinsed with large amount of Milli-Q water, and dried with a gentle nitrogen flow before being stored in a clean and sealed environment.

2.2. Preparation of solutions

For the SAXS and the surface sensitive measurements two different solution preparation protocols were used. The reason for this is that higher lipid concentration is needed for SAXS measurements to yield a good signal-to-noise ratio, and for such measurements the extrusion method was used. Here, DPPC powder was dissolved in chloroform in a small glass vial. Subsequently the solvent was evaporated under a gentle nitrogen flow in order to form a thin lipid film on the glass walls. In order to remove any residual chloroform the vial was placed in a vacuum oven over night (55 °C, 0.1 mbar). 155 mM NaCl solution was added to have a DPPC concentration of 8 mg/mL. The mixture was vortexed and placed in a thermostat shaker for 2 h (55 °C, 300 rpm). Afterwards the solution was passed 35 times through an Avanti mini extruder fitted with a membrane with a pore size of 50 μm. The whole preparation was done at 55 °C, which is well above the phase transition temperature. After this the vesicles were mixed with a hyaluronan solution to yield the final solution with equal hyaluronan and DPPC concentrations of 4 mg/mL.

For the surface sensitive measurements DPPC vesicles were prepared by the sonication method [18]. First the desired amount of DPPC powder was dissolved into a small amount of chloroform (≈0.5 mL). The solvent was then evaporated under a gentle nitrogen flow by rotary evaporation in order to form an even and thin lipid film on the bottle walls. A water jet pump was used to remove any residual chloroform. Next, a 155 mM NaCl solution was added to give a DPPC concentration of 1 mg/mL and the mixture was vortexed for 2 min and then allowed to stand for 1 h at 55 °C. This solution was placed into an ultrasonic bath (Bandelin Sonorex

Digitec, output power 640 W) and sonicated until the dispersion became totally clear. The temperature was kept at 55 °C during the whole preparation process. The average hydrodynamic diameter of the vesicles in 155 mM NaCl containing 0.5 mg/mL DPPC was determined by dynamic light scattering and found to be around 110 nm [6]. Hyaluronan solutions (1 mg/mL) in 155 mM NaCl were prepared one day before the experiment to ensure complete dissolution, and these solutions were stored in a refrigerator. The DPPC and hyaluronan mixture was blended by gently vortexing at 55 °C for 30 min to give a solution containing equal DPPC and hyaluronan concentrations of 0.5 mg/mL. The pH of the mixed solution was measured to be 6.3 ± 0.2. All experiment preparations were done at 55 °C, where the phospholipid chains are in fluid state.

2.3. Instruments and methods

2.3.1. Small angle X-ray scattering (SAXS)

The SAXS measurements were performed at the P12 BioSAXS beamline, PETRA III (EMBL/DESY), Hamburg, Germany. The samples were put in capillaries with a diameter of 1.5 mm and wall thickness 10 μm. The used photon energy was 13 keV. A Linkam heating stage was used for controlling the sample temperature. All measurements were performed at 55 ± 0.1 °C. Measurements of the buffer were used as background and were subtracted from the data. Data have been normalized to transmitted beam [19]. The scattering from the lipid vesicles was modelled by an approach developed by Pabst et al. [20], where the scattered intensity I is described as:

$$I(q) \propto \frac{1}{q^2}|F(q)|^2 S(q), \tag{1}$$

where q is the wave vector transfer which is related to the scattering angle 2ϕ and photon wavelength λ by $q = 4\pi\sin(\phi)/\lambda$. However, this model only accounts for symmetric lipid vesicles whereas in our case one could expect the presence of asymmetric vesicles (vesicles surrounded by a bound hyaluronan layer). Thus, we have modified the formula to account for asymmetric structures. We have omitted the structure factor, $S(q)$, which accounts for the presence of multilamellar vesicles and have instead used two form factors, $F|(q)|^2$; one for a bilayer structure only (unilamellar vesicles) and one for a double bilayer structure. This approach is valid since evaluation of the data showed that only unilamellar and double bilayer structures were present. This simplification of the model made it easy to introduce a further term to account for the asymmetry due to the presence of a hyaluronan layer. Thus the electron density $\rho_{Vesicle\text{-}HA}$ of the asymmetric vesicle structure taken for calculation of F(q) is modelled as:

$$\rho_{Vesicle\text{-}HA} = \rho_i(z) + \rho_{rHA} e^{\frac{-(z-z_{HA})^2}{2\sigma_{HA}^2}}, \quad \text{where} \quad i = s(\textit{for single}),\ d(\textit{for double}) \tag{2}$$

where ρ_s and ρ_d denote the electron density of the single and double bilayer structure, respectively. The relative electron density of the hyaluronan layer is given by ρ_{rHA} and z denotes the position. A detailed compilation of the formula is given in the supporting information.

2.3.2. Quartz Crystal Microbalance with Dissipation (QCM-D)

A quartz crystal microbalance with dissipation monitoring (Q-sense E4, Biolin Scientific, Sweden) was employed to follow adsorption from mixed DPPC/hyaluronan solutions onto AT-cut silica sensors (QSX303, fundamental frequency of 5 MHz, Biolin Scientific, Sweden). The sensors were cleaned by immersion into 2% Hellmanex (Hellma, USA) solution for 30 min, followed by rinsing with a large amount of Milli-Q water. The sensors were subsequently dried using gentle nitrogen flow. The solutions were injected into the measuring chamber by an integrated pump using a flow rate of 150 μL/min. The adsorption was followed at a temperature of 55 °C by monitoring changes in resonance frequency, Δf, and dissipation factor, ΔD. The latter quantity describes the coupling between the sensor and its environment. The data were evaluated using either the Sauerbrey [21] or Voigt [22] model. The Sauerbrey model is applicable when the dissipation is small (normally less than 10^{-6}), whereas the Voigt model is utilised for more dissipating surface layers. In the Voigt model the total stress acting on the film is modelled as an elastic and viscous element coupled in parallel:

$$G^* = G' + jG'' = \mu + j2\pi f\eta \tag{3}$$

Here G' and G'' are the storage and loss modulus respectively, μ is the shear elasticity, η the shear viscosity, f the frequency, and $j = \sqrt{-1}$, as described in more detail elsewhere [22,23,24–26].

Changes in frequency and dissipation recorded for several overtones need to be used when analysing the data, and in this study the 3rd, 5th, and 7th overtones were used. A reasonable value for the layer density ($\rho_1 = 1030$ kg/m^3), and the known values of bulk viscosity ($\eta = 5 \times 10^{-4}$ kg/(sm)) [26], and bulk density ($\rho_2 = 986$ kg/m^3) [27] at the measurement temperature were used to calculate the sensed mass of the layer. We note that this quantity includes the mass of adsorbed DPPC and hyaluronan, as well as the mass of the water that is hydrodynamically coupled to the layer.

2.3.3. AFM force and friction measurement

Forces acting between a silica surface and a silica particle carrying adsorbed layers formed by adsorption from the DPPC/hyaluronan mixture were measured by employing a Multimode Nanoscope III Pico Force atomic force microscope (Bruker, USA). Rectangular tipless cantilevers (CSC12-F, MikroMasch, Estonia) with approximate dimensions of 250 μm in length and 35 μm in width were used in the experiments. The normal (k_N) and torsional (k_Φ) spring constants were determined by utilising the AFM tune IT v2.5 software (Force IT, Sweden) and the thermal noise method [28,29]. A silica particle with a diameter of about 19 μm was glued on top of the cantilever using a two-component epoxy resin (Huntsman, UK), an Eppendorf Micromanipulator 5171 and a Nikon Optiphot 100S reflection microscope. The size of the colloidal probe was determined with the same microscope. Cantilevers with glued particles were cleaned by UV irradiation for 15 min (output 14.76 mW/cm^2, BioForce, US) just before use. The experiments were performed in liquid environment inside a fluid cell (MTFML, Bruker, USA, volume ≈ 100 μL). Care was taken to ensure that the cantilever deflection never exceeded the range where the detector response is close to linear [30]. The desired temperature (47 °C) was obtained by using a heating controller (Veeco, USA), and the surface temperature that corresponded to a given set temperature was determined using a calibration procedure as described previously [5].

2.3.4. AFM imaging

A Dimension FastScan (Bruker, USA) was utilised for recording topographical images of adsorbed layers on silica formed from DPPC/hyaluronan mixtures in 155 mM NaCl at 47 °C. Peak Force Tapping mode was employed for these measurements. A silicon nitride cantilever (Scan Asyst Fluid +, spring constant 0.6 N/m, tip radius 5 nm, Bruker) was used for imaging. The value of the spring constant was determined as described above. A low peak force of 400 pN was used to image the soft adsorbed layer. The experiments were executed in a fluid cell in the following manner: First, the DPPC/hyaluronan mixture was injected and incubated for

40 min. Next a 155 mM NaCl solution was injected to remove non-adsorbed DPPC and hyaluronan. After rinsing, several images were captured at different positions.

3. Results and discussion

In the following, we initially discuss the adsorbing structures that are present in the solution as revealed by SAXS measurements at 55 °C. Next, we report the adsorption from the DPPC/hyaluronan mixture onto silica as monitored by QCM-D. Thereafter, we describe the topography of the adsorbed layer based on AFM imaging, and then present the surface and friction forces acting between such adsorbed layers. These measurements were carried out at 47 °C. At both 55 °C and 47 °C the acyl chains of DPPC is in the fluid state, and the lower temperature in the AFM measurements was chosen due to instrumental restriction.

3.1. Hyaluronan/DPPC vesicle association structures in bulk solution

The structures formed in bulk solution were characterised by SAXS studies of 150 mM NaCl solutions containing DPPC vesicles, hyaluronan, and a mixture of hyaluronan and DPPC vesicles.

Hyaluronan solutions were studied at three different concentrations and the results are shown in Fig. 1. Two asymptotic decays are observed in the solution containing 1 mg/mL hyaluronan. At low q-values a decay typical for a polymer coil is seen and the form factor decreases as $I(q) \sim q^{-2}$. At higher q values the scattering is dominated by smaller length scales and, thus, by the local structure of the polymer chain. Therefore, a crossover to an asymptotic decay proportional to q^{-1} is observed, which is typical for a local rod-like structure [31]. From the location of the crossover at $q^* = 0.118$, the persistence length, L, can be estimated by the relation $L = 6/(\pi q^*)$, yielding a value of 16 nm [31]. This value is in accordance with values found in the literature [31]. With increasing hyaluronan concentration the slope of the scattering curve changes. This is due to overlap of the isolated chains, which leads to formation of an entangled network [32,33]. Thus, the scattering signal is no longer dominated by the signal from the single chains.

The SAXS data for pure vesicles with a concentration of 4 mg/mL are shown in Fig. 2. It has the typical shape for a vesicle in the observed q-regime. Two characteristic humps at $q \sim 1\ \mathrm{nm}^{-1}$ and $q \sim 1.8\ \mathrm{nm}^{-1}$ can be seen, which is a clear sign that the vesicles are not only unilamellar. From the detailed fitting we could estimate that some double bilayer vesicles are present. This is accounted for in the evaluation of the data. Fig. 3 shows the relative electron density profiles obtained by the fitting. The parameters used are reported in Table 1. The distance between the head groups of the DPPC bilayer is evaluated to be 3.6 nm, which is in good agreement with values reported in the literature [34].

Fig. 2 also includes scattering curves of vesicles mixed with hyaluronan. From the comparison of the scattering data of vesicles with and without hyaluronan it can be directly concluded that the repeat distance of the lamellae does not change in presence of hyaluronan. Only a small decrease in the width of the oscillation is present, indicating a broader width of the vesicle outer shell in the presence of hyaluronan; see also Fig. S3 in the supporting information. This data set was modelled with the asymmetric bilayer model as described in the experimental section, Eq. (2). The values extracted from the modelling are given in Table 1. Here the parameters obtained for the vesicles in absence of hyaluronan were fixed and used for the lipid structure also in presence of hyaluronan. Thus, only the additional hyaluronan layer was fitted, yielding good agreement with the data. For comparison the data obtained from the hyaluronan/DPPC vesicles was also modelled without an additional layer of hyaluronan, but this resulted in worse agreement between experiment and model as shown in Fig. S4 of the supporting information. This observation, together with the fact that a satisfactory fit could be achieved by just adding an additional layer that accounts for hyaluronan, is a strong indication that our proposed model of hyaluronan binding to the outer shell of the DPPC vesicles is valid. Furthermore, DLS measurements reported in a previous study suggest that addition of hyaluronan to a DPPC vesicle solution results in an increased hydrodynamic size of the vesicles [6], which is consistent with our finding with SAXS that hyaluronan adsorbs to the outer surface of the vesicles. However, the amount adsorbed is small, suggesting that the surface of the vesicle is not fully covered by hyaluronan.

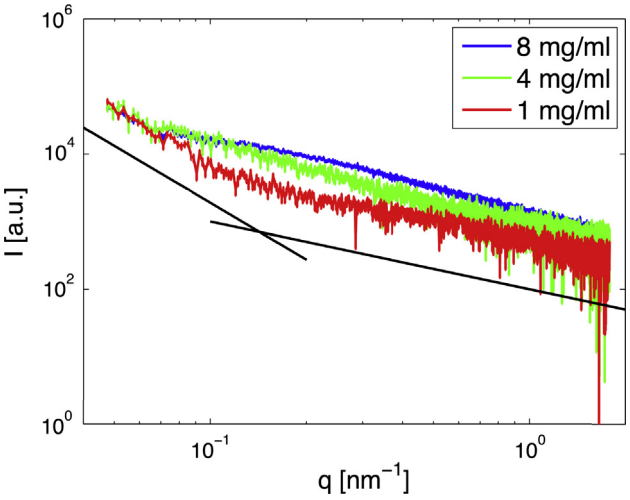

Fig. 1. Small angle scattering curves from 150 mM NaCl solutions containing different concentrations of hyaluronan. Data includes error bars that make the lines thicker. The black lines are guides to the eye and denote an asymptotic decay proportional to −1 and −2, respectively.

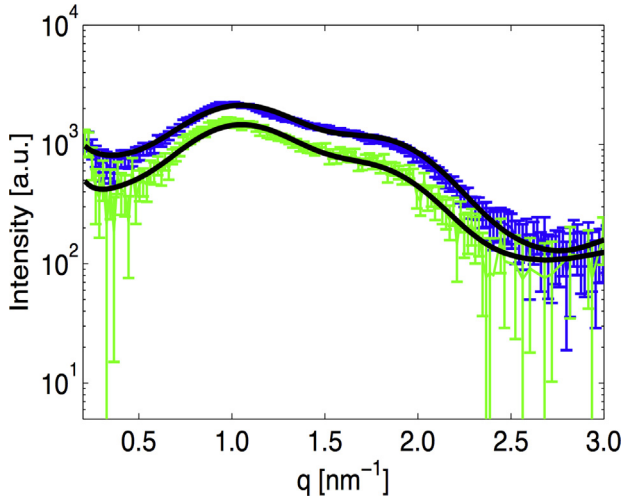

Fig. 2. Scattering curves and fits (black lines) of DPPC vesicles (blue) and DPPC/hyaluronan (HA) vesicles (green). (For interpretation of the references to colour in this figure legend, the reader is referred to the web version of this article.)

3.2. Adsorption from DPPC/hyaluronan mixtures

The adsorption of DPPC vesicles on silica crystal surfaces has been reported in our previous articles [5,6]. We noted an initial peak in frequency and dissipation change after DPPC vesicles injection, indicating adsorption of vesicles followed by vesicle rupture.

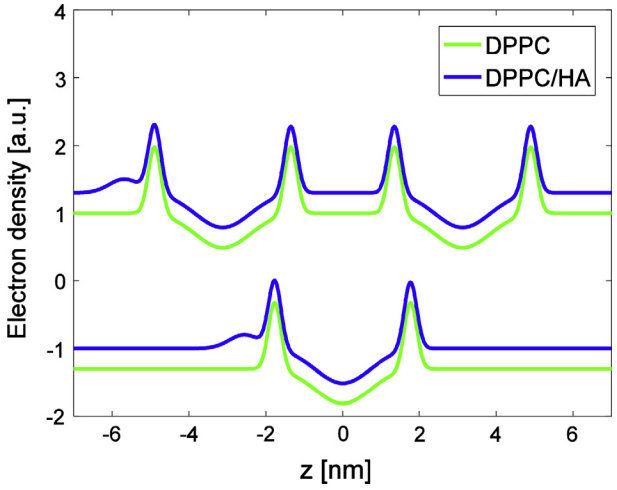

Fig. 3. Electron density profiles of the single DPPC bilayer structure (top) and DPPC double bilayer structure (bottom) in absence (blue) and presence (green) of hyaluronan. (For interpretation of the references to colour in this figure legend, the reader is referred to the web version of this article.)

Table 1
Fitting parameters of the model used for evaluating SAXS data from DPPC vesicles. The width of the headgroup region is given by w_H, which is the full width at half maximum, the width of the tail group region is w_T, the position of the headgroup is z_H (with $z = 0$ being defined to be in the middle of the DPPC bilayer), the contrast is ρ_r, the spacing of the lamellar is d, the fraction of unilamellar vesicles is n, the scattering amplitude at $q = 0$ is A. For the additional HA layer the parameters are the contrast of the hyaluronan, ρ_{HA}, the central position, z_{HA}, and the width of the hyaluronan layer, w_{HA}.

	DPPC vesicles	DPPC/HA vesicles
w_H [nm]	0.42 ± 0.05	0.42 ± 0.05
w_T [nm]	1.90 ± 0.1	1.90 ± 0.1
z_H [nm]	1.80 ± 0.1	1.80 ± 0.1
ρ_r	0.47 ± 0.05	0.47 ± 0.05
d [nm]	6.45 ± 0.5	6.45 ± 0. 5
n	0.85 ± 0.04	0.84 ± 0.04
A	210.00 ± 10	130.00 ± 10
ρ_{rHA}		0.20 ± 0.03
z_{HA} [nm]		2.58 ± 0.2
w_{HA} [nm]		0.91 ± 0.05

After vesicle breakup the frequency change was found to be around −25 Hz and the dissipation increase was less than 1×10^{-6}, consistent with DPPC bilayer formation. In this study, as is shown in the data presented in Fig. 4a, we observe a similar rapid decrease in frequency by −25 Hz after injection of the DPPC/hyaluronan mixture. This suggests that initially a DPPC bilayer forms on the surface, which is consistent with our previous study [6]. However, adsorption does not stop here, but both the magnitude of Δf and ΔD continue to increase with time in a close to linear fashion. The adsorption was allowed to continue for about 100 min, but no tendency of surface saturation was observed. During the rinsing phase, which lasted for 20 min, the frequency and dissipation changes were small, suggesting limited desorption. A second adsorption step was then initiated by injecting the DPPC/hyaluronan mixture again. This resulted in a close to linear change in Δf and ΔD with time, demonstrating continued adsorption.

The dissipation change is plotted versus frequency change in Fig. 4b. Here we only use data from the first adsorption step after the bilayer has formed. A close to linear relation is obtained suggesting that no significant stiffening of the outer layer occurs as the adsorption proceeds. Also shown in Fig. 4b is data from a sequential adsorption experiment where hyaluronan is allowed to adsorb to a preformed DPPC bilayer. In this case the ΔD vs Δf

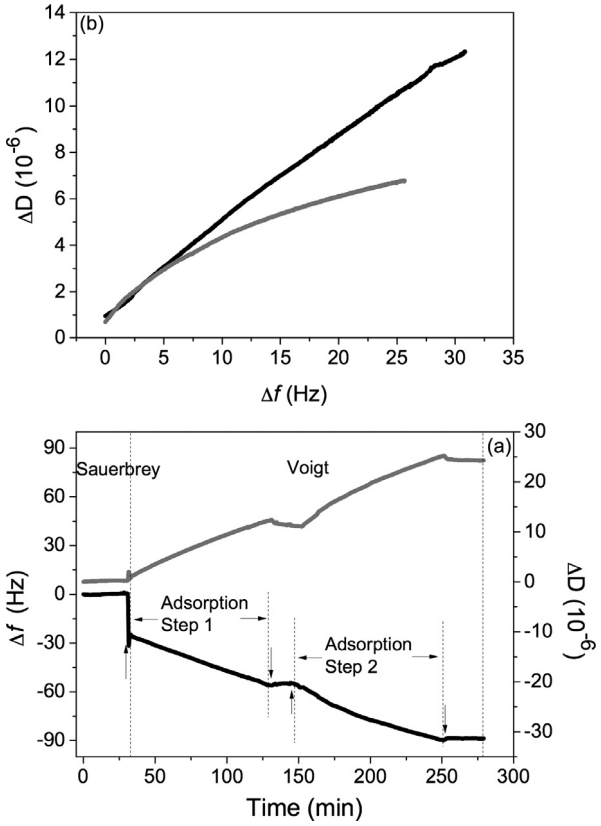

Fig. 4. (a) Adsorption from a solution containing 0.5 mg/mL DPPC and 0.5 mg/mL hyaluronan (start marked by↑) on a silica surface in 155 mM NaCl solution at 55 °C monitored by QCM-D for the 3rd overtone (frequency (black line) and dissipation (grey line) change). Rinsing (start marked by↓) was done with 155 mM NaCl solution at 55 °C. For clarity every 30th point is plotted. (b) Dissipation change versus frequency change during the first adsorption step illustrated in panel a (black line) and data for hyaluronan adsorption on a pre-adsorbed DPPC bilayer (grey line) re-plotted from Ref. [6]. For clarity, only every 7th point is plotted.

curve increases sub linearly, which suggests that the layer stiffens due to repulsive interactions between adsorbed hyaluronan molecules. We also note that for a given value of $\Delta f > 5$ Hz, the value of ΔD is significantly larger for the layer formed from the DPPC/hyaluronan mixture compared to that formed by hyaluronan adsorption on pre-adsorbed DPPC. This suggests that the structures formed by adsorption from the mixture are more extended and viscoelastic.

The sensed mass, which includes the mass of the adsorbing species and associated water, for each adsorption step was calculated, and the results are reported in Table 2. We note that for the initial bilayer formation the Sauerbrey model is appropriate due to the small change in dissipation value. However, large changes in ΔD are observed for the other two adsorption steps, invalidating the Sauerbrey approach. Thus, for these steps we utilised the Voigt model. We note that the sensed mass for the DPPC bilayer, 4.6 ± 0.1 mg/m^2, is close to what has been obtained by adsorption from a DPPC solution containing no hyaluronan, 4.4 ± 0.2 mg/m^2 [5,6]. In Table 2 we also include the state of the layer after 40 min of adsorption since this adsorption time was used for AFM imaging and measurements of surface forces and friction.

3.3. AFM imaging

The surface morphology of the layer formed by adsorption from DPPC/hyaluronan mixtures at 47 °C is shown in Fig. 5. The lateral size of the aggregates present on the surface varies considerably

Table 2
Frequency and dissipation changes recorded by QCM-D and calculated sensed mass for the different regions of the adsorption curve from a DPPC/hyaluronan mixture on silica as illustrated in Fig. 4a. The sensed mass of the DPPC bilayer was calculated using the Sauerbrey model, while for the two following adsorption steps the Voigt model was used.

Adsorption	Sensed mass [mg/m^2]	Sensed mass in total [mg/m^2]
DPPC bilayer	4.6 ± 0.1	4.6 ± 0.1
Adsorption after 40 min	3.3 ± 0.4	7.9 ± 0.4
Adsorption Step 1	9.2 ± 0.2	13.8 ± 0.2
Adsorption Step 2	16.3 ± 2.3	30.1 ± 2.3

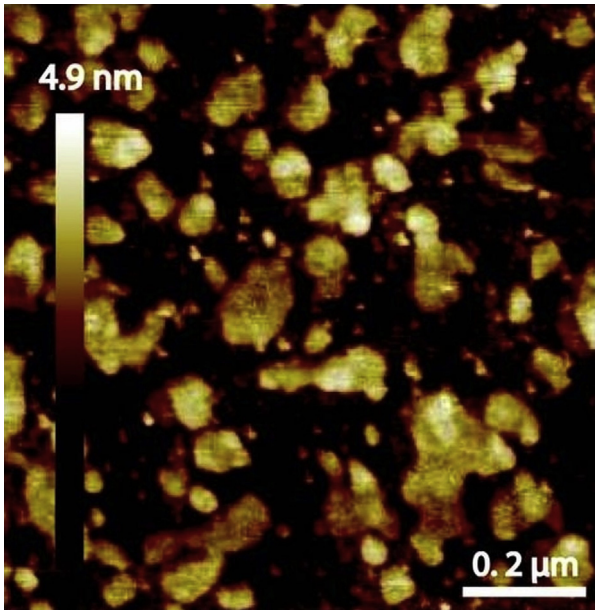

Fig. 5. AFM topography image of the adsorbed layer formed after 40 min adsorption from solutions containing 0.5 mg/mL DPPC and 0.5 mg/mL hyaluronan in 155 mM NaCl on a silica surface. After 40 min the solution was exchanged with pure 155 mM NaCl solution, and the resulting layer was imaged in this solution at a temperature of 47 °C. Image size 1 × 1 µm^2.

in size. Some are considerably smaller than the hydrodynamic diameter of the vesicles found in bulk solution, which is about 140 nm [6], whereas others are of this size. This observation suggests that at least some vesicles fractures on the surface. The low height of the surface features observed by AFM may suggest bilayer aggregates, but considering the soft nature of vesicles we expect considerable deformation during AFM imaging and we can thus not draw the conclusions that no intact vesicles reside on the surface as the height information does not reflect the extension of the aggregates when they are undisturbed by the AFM tip. Indeed, the force curves reported below provide evidence for the presence of some vesicle-like structures on the surface.

3.4. Surface forces

Some examples of force curves measured between silica surfaces after allowing adsorption to proceed for 40 min followed by rinsing with 155 mM NaCl are shown in Fig. 6. Since the adsorbed layer is heterogeneous (see Fig. 5), there is also a variation between forces measured on different spots on the surface.

The typical surface interaction is a long-range repulsion of predominantly steric origin, which increases monotonically with decreasing separation as exemplified in Fig. 6a. This is distinctly

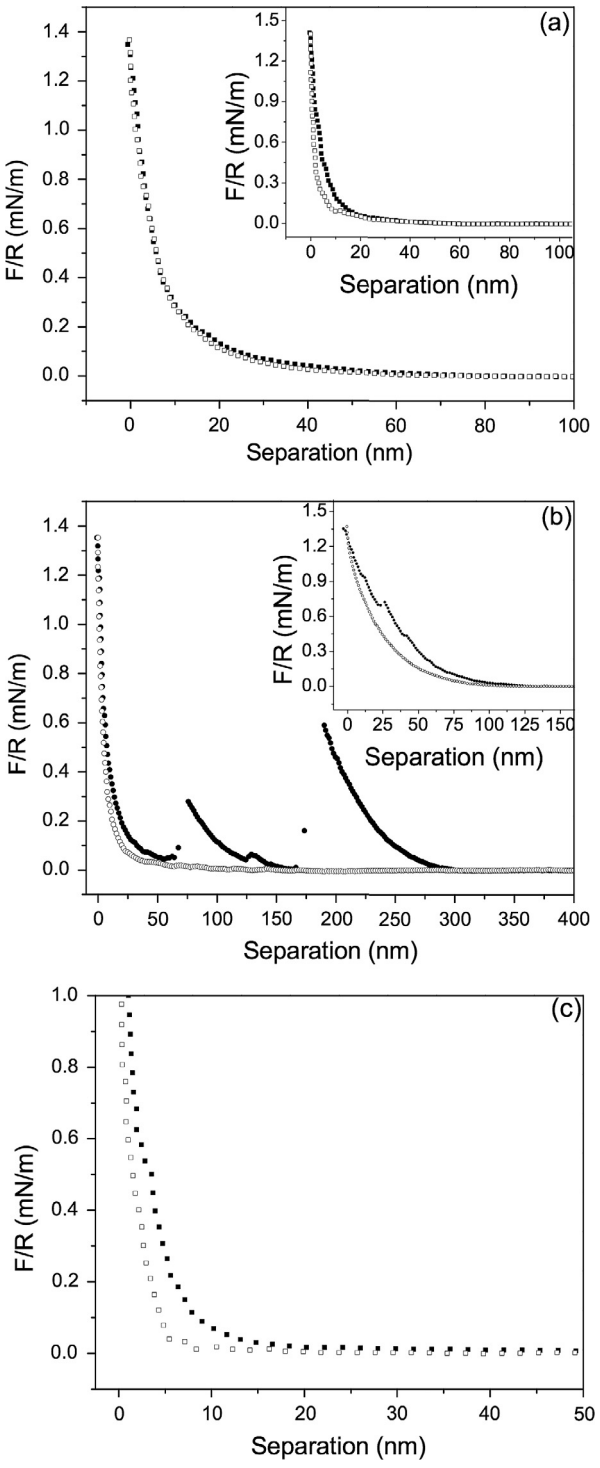

Fig. 6. Force normalised by radius as a function of separation between silica surfaces carrying an adsorbed layer formed from solutions containing 0.5 mg/mL DPPC and 0.5 mg/mL hyaluronan in 155 mM NaCl at 47 °C. The adsorption was allowed to proceed for 40 min before rinsing with 155 mM NaCl, and the forces were recorded after rinsing. (a) Typical force curves recorded before friction (approach (■) and separation (□)) and after friction (inset). (b) Very long range repulsive forces noted on the first approach on one spot (■) before friction measurements. The forces recorded on first separation (□) are also shown. The inset shows the 10th force curve measured on approach (■) and separation (□) on this spot. (c) Force curve measured on approach (■) and separation (□) at the same spot as in panel b after friction measurements.

different compared to the short-range repulsion observed between DPPC bilayers, and more reminiscent of the forces observed when first DPPC and then hyaluronan is adsorbed in sequence [6]. This

suggests that hyaluronan constitutes the outermost layer, which is consistent with the finding that hyaluronan binds to the outer surface of DPPC vesicles, and with previous X-ray reflectivity studies [35].

The structure of the soft DPPC/hyaluronan layer is affected by the friction measurements and these are reported in the next section. In particular, the range of the steric repulsion is decreased after shearing. In the example of Fig. 6a the range of the steric force prior to friction measurements was 60 nm, decreasing to about 40 nm after friction measurements (inset in Fig. 6a). This indicates removal of some of the adsorbed material during the combined action of load and shear. In contrast, no clear evidence of disruption of layer due to consecutive normal force measurements is observed as illustrated in Fig. S5 of the Supplementary Information.

The presence of large aggregates on the surface affected force measurements on a few spots. The most dramatic example is shown in Fig. 6b. Two sets of force curves have been depicted: the approach and separation curves of the first surface force measurement, and those of the 10th measurement (inset). A very long-range repulsive force (up to 300 nm) could be observed in the approach curve of the first force measurement, indicating the presence of a large aggregate. The force increases with decreasing separation until it suddenly returns to zero. We interpret this as deformation of the aggregate followed by a sudden rearrangement into another structure. The process repeats as the separation is decreased further, and another force maximum is experienced followed by a rearrangement within the adsorbed layer. Less dramatic changes in layer structure is observed upon consecutive force measurements as exemplified by the 10th surface force measurement reported in the inset of Fig. 6b. Upon compressions a few small steps are noted, where each step size roughly corresponds to the thickness of a DPPC bilayer. Thus, the large aggregate that initially was present on the surface is being transformed into a multilayer structure by consecutive compressions. We note that similar structural forces have been observed in synthetic polyelectrolyte-surfactant systems [36–38].

The force curves measured after friction measurement on the spot corresponding to the data reported in Fig. 6b are shown in Fig. 6c. The long-range repulsive force observed prior to friction measurements (Fig. 6b) is now absent. Instead, the force curves measured are similar to those determined after friction measurements on a typical spot (Fig. 6a, inset). Clearly, the range of the repulsive force is significantly larger in the case of the DPPC/hyaluronan mixture than observed between DPPC bilayers formed in absence of hyaluronan [6], and more similar to what is observed for sequential adsorption of DPPC and hyaluronan [6]. Thus, it can be concluded that the remaining layer after shearing is not a pure DPPC bilayer but more likely a DPPC bilayer with hyaluronan on top.

3.5. Friction forces

In the previous sections we have shown that adsorption from mixed solutions of DPPC and hyaluronan results in formation of an inhomogeneous layer, in stark contrast to the more even layers formed by sequential adsorption of these two components [6]. Intuitively, one could expect that the friction force would be large as two such rough surfaces are sheared against each other. However, the friction forces measured between the inhomogeneous layers formed from the DPPC/hyaluronan mixture instead turns out to be very low as shown in Fig. 7(a). The average friction force and the standard deviation were obtained from about 96 friction loops at each normal load, carried out at three different spots. Within experimental uncertainty the same average friction vs. load curve were obtained on loading and unloading.

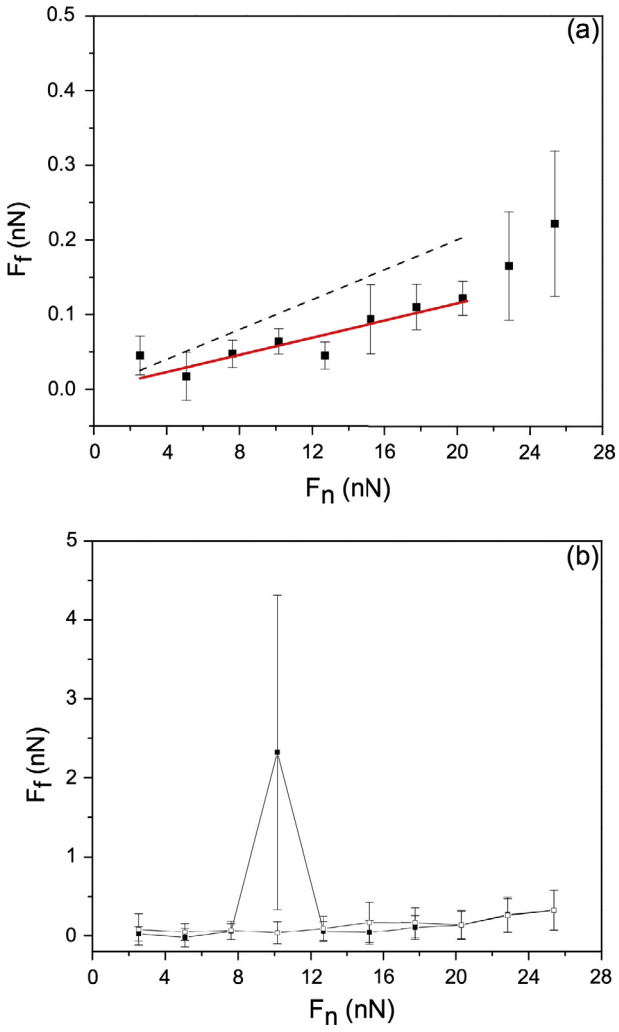

Fig. 7. (a) Friction force as a function of load between two silica surfaces carrying an adsorbed layer formed after 40 min adsorption from a 155 mM NaCl solution containing 0.5 mg/mL DPPC and 0.5 mg/mL hyaluronan, followed by rinsing (■). The temperature was 47 °C. The solid line has a slope of 0.006 and the slope of the dashed line is 0.01. (b) Illustration of one of the three friction measurements depicting high friction force at a normal force of 10 nN upon loading.

The maximum load used in this study can be converted to pressure using the Hertz model [39], and it was found to be around 23 MPa. This is close to the critical pressure that a cartilage surface can withstand before it breaks under axial load [40].

At low loads, up to a load of roughly 20 nN, Amonton's rule stating that the friction force, F_f, is proportional to the normal load, F_n, describes the data well.

$$F_f = \mu F_n \tag{4}$$

Here μ is the friction coefficient. The best fit to the data in this load regime, corresponding to the red[2] line in Fig. 7(a), returns a value of the friction coefficient as low as 0.006. For comparison a dashed line corresponding to a friction coefficient of 0.01 is also shown in Fig. 7(a). The low friction force obtained in this study is comparable to that reported for synovial joints [4]. That such a low friction force can be obtained between initially inhomogeneous surface layers strongly suggests that the layers rearrange under the combined action of load and shear, and transform into phospholipid

[2] For interpretation of color in Fig. 7, the reader is referred to the web version of this article.

bilayer or multilayer structures separated by easily sheared water layers. This suggestion is supported by the difference in normal forces observed before and after friction measurements (see Fig. 6). It is the presence of strong hydration and entropic protrusion forces between DPPC bilayers [41] that stabilises a thin water layer and facilitates sliding with a low friction force. Low friction forces have also been reported for surfaces coated with DPPC bilayers [17,6] and phospholipid liposomes [42], and thus hyaluronan is not essential for achieving the low friction force. A study of friction between cartilage surfaces in presence of mixtures of DPPC, hyaluronan and lubricin has also been reported, and here the key role of the biomacromolecules was emphasised [43].

An observation of interest, which occurred in some cases, is shown in Fig. 7(b). At a given applied load, around 10 nN in the case shown, there is a sharp and transient increase in the obtained friction force value. We assign it to energy dissipation due to structural rearrangement induced by load and shear. Thus, just as disruption and rearrangement can occur during measurements of surface forces (Fig. 6b), such structural rearrangements occur during friction measurements where they give rise to transient friction peaks. This phenomenon has also been reported for a system containing a cationic polyelectrolyte and an anionic surfactant [38]. When such a peak was observed, it was noted that out of the 16 scans performed at this particular load there were only 1–3 consecutive scans showing relatively high friction. This is the reason for high standard deviation at the load where the friction peak is observed. The transient high value of friction observed at the friction peak was not included in the average value reported in Fig. 7(a).

It is important to note here that the layer is able to continue to provide low friction after the rearrangement that gives rise to the friction peak. This is distinctly different from that of a DPPC bilayer (without hyaluronan), which when compromised during a friction vs. load measurement remains in a high friction state during the rest of the measurement [17]. Thus, the DPPC hyaluronan mixture provides lubrication synergy as opposed to lone DPPC bilayers. The presence of hyaluronan allows accumulation of larger quantities of phospholipids at the interface. This facilitates return to a low friction state after disruption of the original layer structure under load and shear. We also note that DPPC and hyaluronan are not unique, but a similar lubrication self-healing has been reported for a mixture of a cationic polyelectrolyte and an anionic surfactant [38].

In summary, hyaluronan associates with DPPC vesicles in bulk solution, and during adsorption to silica surfaces DPPC-hyaluronan aggregates form on top of a DPPC bilayer. Upon the combined action of load and shear these aggregates can be deformed and disrupted. However, the mixed adsorbed layer provides very low friction forces up to a pressure of 23 MPa, even though transient friction peaks are observed during layer rearrangements. It is imperative to stress that the presence of the DPPC/hyaluronan aggregates constitutes a surface bound reservoir for the phospholipid lubricant, which facilitates return to a low friction state after shear and load induced structural changes in the layer.

4. Conclusions

Biolubrication involves a range of molecular structures, including bottle-brush polymers such as mucins and lubricins as well as linear polysaccharides and low molecular weight phospholipids that work in synergy [2,3,4–6,8,9]. It has previously been shown that phospholipid liposomes [44] and sequential adsorption of DPPC and hyaluronan [6] result in layers that provide low friction force in aqueous media. However, in a fluid containing both DPPC and hyaluronan it is more likely that self-assembly structures first form in solution and then adsorb to the surface. In this work we explore the structure and lubrication performance of such layers. Our data on the solution structure of the hyaluronan/DPPC mixture indicates binding of hyaluronan to the outer shell of the DPPC vesicles. In this association process the vertical structure of the lipid bilayer is not changed and the spacing between bilayers is the same as in absence of hyaluronan. The data obtained by QCM-D suggests that a DPPC bilayer is rapidly established on the silica surface, and thereafter a slow adsorption of DPPC/hyaluronan aggregates follows. As a consequence, the layer formed by adsorption from the DPPC/hyaluronan mixture is inhomogeneous, in stark contrast to layers formed from DPPC solutions without hyaluronan and during sequential adsorption of DPPC and hyaluronan. Importantly, the inhomogeneous nature of the initially formed layer does not compromise the lubrication performance. Rather the aggregates are easily compressed and disrupted during surface force and friction measurements as shown by distinct force maxima (Fig. 6) during compressions and transient friction peaks (Fig. 7) during shearing. Our data show that the layers readily transform to structures that promote low friction, suggesting phospholipid bilayer and multilayer structures containing easily sheared water layers. Indeed, the friction force between the layers formed by adsorption from DPPC/hyaluronan mixtures is very low and consistent with that found between DPPC bilayers [6]. In previous work low friction forces have also been reported for synthetic cationic polyelectrolytes exposed to anionic surfactants [38]. We note that the layers formed by adsorption of DPPC/hyaluronan self-assembly structures provide a lubrication advantage over that of DPPC alone by possessing self-healing ability. This is due to the presence of DPPC/hyaluronan aggregates on the surface that allows the build-up of a reservoir of the lubricating phospholipids on the solid surfaces. Clearly, the inhomogeneous DPPC/hyaluronan layer formed by adsorption of self-assembly structures of these components provides excellent lubrication, and if such layers are also present on natural surfaces, favourable lubrication properties can be expected. Further studies focusing on lubrication synergy between additional biolubricants would clearly advance our understanding of biolubrication processes.

Acknowledgements

MW acknowledges a stipend from China Scholarship Council (CSC). AR acknowledges funding from the People Programme (Marie Curie Actions) of the European Union's Seventh Framework Programme FP7/2007-2013/ under REA grant agreement n 290251. We gratefully acknowledge technical support from Clement Blanchet (EMBL) at the P12 BioSAXS beamline (EMBL/DESY, PETRA III). We wish to acknowledge the financial support by the BMBF-project 05K2012 within the Joint International Research Project Röntgen-Angström-Cluster.

Appendix A. Supplementary material

Supplementary data associated with this article can be found, in the online version, at http://dx.doi.org/10.1016/j.jcis.2016.10.091.

References

[1] M. Huber, S. Trattnig, F. Lintner, Anatomy, biochemistry, and physiology of articular cartilage, Invest. Radiol. 35 (10) (2000) 573–580.
[2] A. Dėdinaitė, Biomimetic lubrication, Soft Matter 8 (2) (2012) 273–284.
[3] B. Hills, Surface-active phospholipid: a Pandora's box of clinical applications. Part II. Barrier and lubricating properties, Int. Med. J. 32 (5–6) (2002) 242–251.
[4] J. Klein, Molecular mechanisms of synovial joint lubrication, Proc. Inst. Mech. Eng., Part J: J. Eng. Tribol. 220 (8) (2006) 691–710.
[5] C. Liu, M. Wang, J. An, E. Thormann, A. Dedinaite, Hyaluronan and phospholipids in boundary lubrication, Soft Matter 8 (40) (2012) 10241–10244.

[6] M. Wang, C. Liu, E. Thormann, A. Dėdinaitė, Hyaluronan and phospholipid association in biolubrication, Biomacromolecules 14 (12) (2013) 4198–4206.
[7] B. Zappone, G.W. Greene, E. Oroudjev, G.D. Jay, J.N. Israelachvili, Molecular aspects of boundary lubrication by human lubricin: effect of disulfide bonds and enzymatic digestion, Langmuir 24 (4) (2008) 1495–1508.
[8] J. Seror, L.Y. Zhu, R. Goldberg, A.J. Day, J. Klein, Supramolecular synergy in the boundary lubrication of synovial joints, Nat. Commun. 6 (2015).
[9] S. Jahn, J. Seror, J. Klein, Lubrication of articular cartilage, Annu. Rev. Biomed. Eng. 18 (2016) 235–258.
[10] E.A. Balazs, D. Watson, I.F. Duff, S. Roseman, Hyaluronic acid in synovial fluid. I. Molecular parameters of hyaluronic acid in normal and arthritic human fluids, Arthritis Rheum. 10 (4) (1967) 357–376.
[11] R. Kohn, P. Kovac, Dissociation-constants of d-galacturonic and d-glucuronic acid and their o-methyl derivatives, chemicke zvesti 32 (4) (1978) 478–485.
[12] R. Tadmor, N.H. Chen, J. Israelachvili, Normal and shear forces between mica and model membrane surfaces with adsorbed hyaluronan, Macromolecules 36 (25) (2003) 9519–9526.
[13] R.W. Forsey, J. Fisher, J. Thompson, M.H. Stone, C. Bell, E. Ingham, The effect of hyaluronic acid and phospholipid based lubricants on friction within a human cartilage damage model, Biomaterials 27 (26) (2006) 4581–4590.
[14] A.V. Sarma, G.L. Powell, M. LaBerge, Phospholipid composition of articular cartilage boundary lubricant, J. Orthop. Res. 19 (4) (2001) 671–676.
[15] L.R. Gale, Y. Chen, B.A. Hills, R. Crawford, Boundary lubrication of joints: characterization of surface-active phospholipids found on retrieved implants, Acta Orthop. 78 (3) (2007) 309–314.
[16] S. Tristram-Nagle, J.F. Nagle, Lipid bilayers: thermodynamics, structure, fluctuations, and interactions, Chem. Phys. Lipids 127 (1) (2004) 3–14.
[17] M. Wang, T. Zander, X.Y. Liu, C. Liu, A. Raj, D.C.F. Wieland, V.M. Garamus, R. Willumeit-Romer, P.M. Claesson, A. Dedinaite, The effect of temperature on supported dipalmitoylphosphatidylcholine (DPPC) bilayers: structure and lubrication performance, J. Colloid Interface Sci. 445 (2015) 84–92.
[18] S.H. Kim, E.I. Franses, New protocols for preparing dipalmitoylphosphatidylcholine dispersions and controlling surface tension and competitive adsorption with albumin at the air/aqueous interface, Colloidal Surf. B: Biointerfaces 43 (3-4) (2005) 256–266.
[19] D. Franke, A.G. Kikhney, D.I. Svergun, Nucl. Instruments Methods Phys. Res. Sect. A (2012) 52–59.
[20] G. Pabst, R. Koschuch, B. Pozo-Navas, M. Rappolt, K. Lohner, P. Laggner, Structural analysis of weakly ordered membrane stacks, J. Appl. Crystallogr. 36 (2003) 1378–1388.
[21] G. Sauerbrey, Verwendung von Schwingquarzen zur Wägung dünner Schichten und zur Mikrowägung, Z. Phys. 155 (1959) 206.
[22] M.V. Voinova, M. Rodahl, M. Jonson, B. Kasemo, Viscoelastic acoustic response of layered polymer films at fluid-solid interfaces: continuum mechanics approach, Phys. Scripta 59 (5) (1999) 391–412.
[23] J. Iruthayaraj, G. Olanya, P.M. Claesson, Viscoelastic properties of adsorbed bottle-brush polymer layers studied by quartz crystal microbalance – dissipation measurements, J. Phys. Chem. C 112 (38) (2008) 15028–15036.
[24] S.X. Liu, J.T. Kim, Application of Kevin—Voigt model in quantifying whey protein adsorption on polyethersulfone using QCM-D, J. Assoc. Lab. Automat. 14 (4) (2009) 213–220.
[25] F. Höök, M. Rodahl, P. Brzezinski, B. Kasemo, Energy dissipation kinetics for protein and antibody−antigen adsorption under shear oscillation on a quartz crystal microbalance, Langmuir 14 (4) (1998) 729–734.
[26] C.T. Nguyen, F. Desgranges, G. Roy, N. Galanis, T. Maré, S. Boucher, H. Angue Mintsa, Temperature and particle-size dependent viscosity data for water-based nanofluids – hysteresis phenomenon, Int. J. Heat Fluid Flow 28 (6) (2007) 1492–1506.
[27] G.S. Kell, Density, thermal expansivity, and compressibility of liquid water from 0 degrees to 150 degrees – correlations and tables for atmospheric-pressure and saturation reviewed and expressed on 1968 temperature scale, J. Chem. Eng. Data 20 (1) (1975) 97–105.
[28] C.P. Green, H. Lioe, J.P. Cleveland, R. Proksch, P. Mulvaney, J.E. Sader, Normal and torsional spring constants of atomic force microscope cantilevers, Rev. Sci. Instrum. 75 (6) (2004) 1988–1996.
[29] J.E. Sader, J.W.M. Chon, P. Mulvaney, Calibration of rectangular atomic force microscope cantilevers, Rev. Sci. Instrum. 70 (10) (1999) 3967–3969.
[30] E. Thormann, T. Pettersson, P.M. Claesson, How to measure forces with atomic force microscopy without significant influence from nonlinear optical lever sensitivity, Rev. Sci. Instrum. 80 (9) (2009) 093701.
[31] E. Buhler, F. Boue, Chain persistence length and structure in hyaluronan solutions: ionic strength dependence for a model semirigid polyelectrolyte, Macromolecules 37 (4) (2004) 1600–1610.
[32] A.L. Kjoniksen, K.Z. Zhu, M.A. Behrens, J.S. Pedersen, B. Nystrom, Effects of temperature and salt concentration on the structural and dynamical features in aqueous solutions of charged triblock copolymers, J. Phys. Chem. B 115 (10) (2011) 2125–2139.
[33] J.S. Pedersen, C. Svaneborg, K. Almdal, I.W. Hamley, R.N. Young, A small-angle neutron and X-ray contrast variation scattering study of the structure of block copolymer micelles: corona shape and excluded volume interactions, Macromolecules 36 (2) (2003) 416–433.
[34] J.F. Nagle, S. Tristram-Nagle, Structure of lipid bilayers, Bba-Rev. Biomembr. 1469 (3) (2000) 159–195.
[35] T. Zander, D.F. Wieland, A. Raj, M. Wang, B. Nowak, C. Krywka, A. Dėdinaitė, P. M. Claesson, V.M. Garamus, A. Schreyer, The influence of hyaluronan on the structure of a DPPC—bilayer under high pressures, Colloids Surf., B 142 (2016) 230–238.
[36] P.M. Claesson, A. Dedinaite, E. Blomberg, V.G. Sergeyev, Polyelectrolyte-surfactant association at solid surfaces, Ber. Bunsenges. Phys. Chem. 100 (6) (1996) 1008–1013.
[37] A. Dedinaite, P.M. Claesson, M. Bergström, Polyelectrolyte-surfactant layers: adsorption of preformed aggregates versus adsorption of surfactant to preadsorbed polyelectrolyte, Langmuir 16 (12) (2000) 5257–5266.
[38] A. Dedinaite, T. Pettersson, B. Mohanty, P.M. Claesson, Lubrication by organized soft matter, Soft Matter 6 (7) (2010) 1520–1526.
[39] H. Hertz, J. Reine Angew. Math. 92 (1881) 156.
[40] G. Spahn, R. Wittig, Biomechanical properties (compressive strength and compressive pressure at break) of hyaline cartilage under axial load, zentralblatt fur chirurgie 128 (1) (2003) 78–82.
[41] J. Israelachvili, H. Wennerstrom, Role of hydration and water structure in biological and colloidal interactions, Nature 379 (6562) (1996) 219–225.
[42] R. Goldberg, A. Schroeder, Y. Barenholz, J. Klein, Interactions between adsorbed hydrogenated soy phosphatidylcholine (HSPC) vesicles at physiologically high pressures and salt concentrations, Biophys. J. 100 (10) (2011) 2403–2411.
[43] T.A. Schmidt, N.S. Gastelum, Q.T. Nguyen, B.L. Schumacher, R.L. Sah, Boundary lubrication of articular cartilage – role of synovial fluid constituents, Arthritis Rheum. 56 (3) (2007) 882–891.
[44] R. Goldberg, A. Schroeder, G. Silbert, K. Turjeman, Y. Barenholz, J. Klein, Boundary lubricants with exceptionally low friction coefficients based on 2D close-packed phosphatidylcholine liposomes, Adv. Mater. 23 (31) (2011) 3517.